Proceedings of the Korean Nuclear Society Spring Meeting
Kwangju, Korea, May 2002

A Photographic Study on Flow Boiling of R-134a in a Vertical Channel

In Cheol Bang[1], Won-Pil Baek[2] and Soon Heung Chang[1]

[1]Korea Advanced Institute of Science and Technology
373-1, Guseong-dong , Yuseong-gu, Daejeon, Korea, 305-701

[2]Korea Atomic Energy Research Institute
150, Dukjin-dong, Yuseong-gu, Daejeon, Korea,305-353

Abstract

The behavior of near-wall bubbles in subcooled flow boiling has been investigated photographically for R134a flow in vertical, one-side heated and rectangular channels at mass fluxes of 0, 190, 1000 and 2000 kg/m^{2}s and inlet subcooling condition of 8 ^{o}C under 7 bar(Tsat 27 ^{o}C). Digital photographic techniques and high-speed camera are used for the visualization, which have significantly advanced for recent decades. Primary attention is given to the bubble coalescence phenomena and the structure of the near-wall bubble layer. At subcooled and low-quality conditions, discrete attached bubbles, sliding bubbles, small coalesced bubbles and large coalesced bubbles or vapor clots are observed on the heated surface as the heat flux is increased from a low value. Particularly in beginning of vapor formation, vapor remnants below discrete bubble on the heating surface are clearly observed. Nucleation site density increases with the increases in heat flux and channel-averaged enthalpy, while discrete bubbles coalesce and form large bubbles, resulting in large vapor clots. Waves formed on the surface of the vapor clots are closely related to Helmholtz instability. At CHF occurrence it is also observed that wall bubble layer beneath large vapor clots is removed and large film boiling occurs. Through the present visual test, it is observed that wall bubble layer begins to develop with the onset of nucleate boiling(ONB) and to extinguish with the occurrence of the CHF. It could be considered that this layer made an important role of CHF mechanism macroscopically. However, there may be another structure beneath wall bubbles which supplies specific information on CHF from viewpoint of microstructure based upon the observation of the liquid sublayer beneath coalesced bubbles. Through this microscopic visualization, it may be suggested that the following flow structures characterize the flow boiling phenomena : (a) vapor remnants as a continuous source of bubbles, (b) liquid sublayer depleted with bubble formation if there is not new supply of liquid, and (c) vapor clot as an obstructer blanketing liquid supply to sublayer in

high heat flux.

1. Introduction

There is a boundary of the effective nucleate boiling heat transfer regime, called the departure from nucleate boiling (DNB). Reliable understanding of this DNB phenomenon is important for effective and safe operation of nuclear systems and other thermal-hydraulic equipment. Detailed physical mechanisms leading to DNB, however, have not been clearly understood in spite of extensive research, mainly due to the difficulty in observing the near-wall region. Particularly, visualization experiments using water with high pressure and high temperature conditions to understand the DNB phenomenon of water cooled reactor well are very difficult and did not give the clear information. Therefore, using of R134a as a modeling fluid with the similar flow characteristics has many merits in a visual study for understanding a mechanism owing to its low critical pressure and vaporization heat. The advanced visual studies on the nucleate boiling regime may supply important clues and basic information on flow structure in boiling and related to the bubble behavior. Gunther [1] for water showed that an increase of heat transfer rate causes bubble population to increase up to a limit where bubbles coalesce to vapor clumps and bubble coalescence signifies incipient film boiling and burnout. Jiji and Clark [2] for water and rectangular channel showed that the bubble boundary layer thickness increased with increasing distance from the leading edge by an increase in bubble size and a thin layer of superheated vapor is formed over the heated surface as the maximum heat flux is approached. Del Valle and Kenning [3] reported that the flow regime changed from bubbly flow regime to slug flow one in decrease of subcooling for water rectangular channel. Tong et al. [4] identified the effect of mass flow rate on bubble size and correlated the bubble size for R113 fluid. Galloway and Mudawar [5] reported that vapor bubbles coalesce into large vapor waves at high heat flux in using FC-87 fluid and rectangular channel. Recently, Yin et al. [6] provided empirical correlations for the boiling heat transfer and for the bubble departure diameter in the subcooled flow boiling, and visualized the bubble characteristics for R134a in a horizontal annular duct at low mass fluxes. Digital photographic techniques have significantly advanced for recent decades. This would enable researchers to overcome some difficulties of visualization study in relation to complex and microscopic boiling phenomena with the easiness of test and high spatial resolution [7][8]. In this study, by using digital photographic techniques, boiling characteristics and flow structure have been examined for the flow boiling of R134a in a vertical rectangular channel with one-side heating.

2. Experimental Method

2.1. Experimental Loop and Test Section

Subcooled flow boiling tests have been performed at pressure of 7 bar (Tsat 27 ^{o}C) for mass fluxes of 0, 190, 1000, 2000 kg/m^{2}s and inlet subcooling conditions of 8 ^{o}C for R134a

fluid.

Figure 1 shows the R134a experimental loop that consists of the following components: an accumulator for pressure control, a non-seal canned pump for stable mass supply, a mass flow-meter with high accuracy, a pre-heater for inlet subcooling control, a test section for visualization, a condenser with phase change, a chiller or chilling system with R22 and water-propylene glycol. A chillier contains a heat exchanger for R134a cooling with water-propylene glycol flow that is cooled in a bath with R22 refrigeration system. Electrical power is supplied by DC power supply HP 6680A with the maximum capacity of 4.375 KW (5V, 875A).

A vertical, one-side heated rectangular channel has been used as the test section as shown in figure 2. It consists of two components: a channel body and an inserter containing a heating plate. In addition, the lower part with an entrance length over than 40 times the channel hydraulic diameter provides fully developed turbulent flow. The body is made of aluminum alloy and provides a flow channel of 8 mm(width including the heated surface)x5 mm (height with window), and polycarbonate windows for visualization from front and side parts. The inserter is made of Bakelite as an insulator and a stainless steel heating plate with the size of 4 mm (width) x 100 mm (length) x 1.9 mm (thickness). The plate is heated by the DC power that is supplied through copper electrodes connected at both ends. The Bakelite insulator assures sufficient insulation allowing only a negligible heat loss to the surrounding air. To measure the heater surface temperature, two type K thermocouples are embedded in the heating plate of Inconel 600 at the positions of 1 mm and 9 mm from the leading edge (i.e., the top of the heated section), and 0.4 mm in depth from the heated surface. The loop is filled with R134a in the vacuum.

2.2. Visualization Method

Visualization of the flow channel in this study has been achieved by the aid of a Nikon D1 digital camera with total 2.74 million pixels(record pixels 2000x1312 which is used really) as a still camera and flash-synchronized shutter speed of 1/500 second with considering the speed and advanced image resolution, which provide the spatial resolution of ~10 μm per pixel to the images of this visual test. Figure 3 shows the photographic system.

Photographic technique that controls the exposure time by the flash speed is adopted for acquiring the clear still image of fast bubbles and disturbed boiling states. While the shutter is open, a high-speed flash of 1/8700 second is emitted to the flow channel. Additional backlighting is provided through a tracing paper in cases of lateral observation. The light source is a Nikon Speedlight SB-28 model. Nikon 105 mm micro lens and three extension tubes of 14 mm, 21 mm and 31 mm for close-up have been used to magnify the phenomena occurring in the flow channel. The focusing of the camera is fixed on the heating surface for front observation and the middle point of the flow width for side observation. After the capture of a bubble motion, image processing is performed mainly on the brightness and contrast of an image.

3. Results and Discussion

Visualization of the near-wall region has enabled to identify the flow structure up to the

range of several tens of microns. Simultaneous front and lateral observations were tried first, but it provided low-quality photographs due to the difficulty in providing proper lighting for both directions. Therefore, front observation was made first and lateral observation followed at similar conditions. The photographs obtained in this work have different characteristics according to the method of lighting even for the same conditions of mass flux, heat flux and subcooling. For example, back lighting and front lighting give clear images for near-wall (i.e., stationary) bubbles while lateral lighting for flowing bubbles. The overlapping of flowing bubbles and vapor clots over the heated surface gives the disorder to the spatial depth.

3.1 Boiling Curves and Experimental Conditions

The boiling curves measured in experiment are shown in figure 4. The heat flux was estimated directly from the applied power. The inner surface temperature was roughly estimated to the measured temperature at 0.4 mm distance from the surface(or heated surface temperature means the measured one.). These curves certainly show the difference of heat transfer capacity among flow regimes.

3.2 Overall Bubble Behavior on the Heated Surface

Overall Boiling Phenomena at Lower Mass Fluxes

Figure 5 shows pool boiling on overall heated surface. As heat flux increase, bubbles' formations on the surface are violent while bubbles coalesces with each other and their agglomeration form slug bubbles or large vapor clot at bulk flow. On the other hands, if a little mass flow of R134a liquid is given, bulk flow phenomena are changed. Bubble layer becomes smaller and bubbles' coalescences occur near and along heated wall as seen in figure 6. Therefore, an effect of mass flux is related to suppression of bubble coalescence and bubble layer growth. Both of figure 5 and 6 show vertically flowing bubbles at zero liquid flow and low one. From the observations, bubbly layer or bubble fraction in bulk flow have thicker and is earlier developed in pool boiling than low flow boiling. These overall boiling phenomena can provide the similar trend or apparently reliable similarity between R134a as a modeling fluid and water as an original fluid.

Boiling Phenomena at Higher Mass Fluxes

Figure 7 shows the boiling phenomena at higher mass fluxes. At low heat flux, discrete bubbles are formed and as the increase of heat flux, bubbles begin to coalesce with each other. In the case of this test, an outstanding phenomenon is near-wall layer of small bubbles which are continuously growing beneath large coalesced bubbles. This layer is a source of large vapor clots in liquid core.

The coalescence phenomena are similar with the case of water boiling[9]. Front observations of figure 7 (a),(c) show large vapor clots above small bubbles near wall and another their merging with heat flux increase. While boiling, bubbles on heated surface seems like a carpet on the floor(heated surface). The coalescence of bubbles occurs in two ways: (i) coalescing of some bubbles growing at neighboring nucleation sites, and (ii) merging of

bubbles growing at nucleation sites into the larger flowing bubbles.

Lateral observations of figure 7 (b), (d) show specific relations between wall bubbles and large vapor clots. It is considered that wall bubbles are a major source of forming large vapor clots. It is also considered that large vapor clots have a limitation of growth or size due to Helmholz instability that is related to waves observed on the surface of the vapor clots. This is very closely linked to CHF phenomena as seen in figure 7 (c) and figure 8.

3.3 Bubble Behavior near CHF Condition

Figure 8 shows the phenomena in CHF conditions for mass flux of 2000 kg/m^{2}s. Wall bubbles layer beneath large vapor clots is removed and large film boiling occurs. This film boiling is observed locally with some distance with the size of vapor clot. Interactions of vapor clots and wall bubble layer just before CHF seems to be an important factor on CHF mechanism. Figure 8 (a) and (b) like figure 7 (c) show the limitation of size of large vapor clots just before and at CHF. After CHF, large vapor clots form one overall film carpet of vapor. There are no longer carpets of wall bubbles beneath vapor clots.

3.4 Identification of Flow Structure

Through the present visual test, it is observed that wall bubble layer begins to develop with the onset of nucleate boiling (ONB) and to extinguish with the occurrence of the CHF. We can consider that this layer make an important role of CHF mechanism macroscopically. However, there may be other structures beneath wall bubble which supply specific information on CHF from viewpoint of micro-strucutre. Second photo of figure 9 shows the liquid layer beneath coalesced bubble. The thin layers below coalesced bubbles are considered as the liquid sublayer that is assumed in many CHF modeling, e.g., Lee and Mudawwar [10], Katto [11] and Celata et al. [12].

Additionally, more microscopic structures of discrete bubble, such as vapor remnant [13], bubble growth and detachment in figure 10 and 11 are shown for low heat flux, which cannot be observed due to complex boiling in case of high heat flux. Second photo in figure 10 (b) shows very tiny bubbles on the heated wall which may be considered as initiating nucleation.

It may be suggested that the following flow structures characterize the flow boiling phenomena. : (i) vapor remnants as a continuous source of bubbles, (ii) liquid sublayer depleted with bubble formation if there is not new supply of liquid, and (iii) vapor clot as an obstructer blanketing liquid supply to sublayer in high heat flux. For this, further work would be required for different pressure, subcooling and mass flux conditions with refrigerants. Visualization equipment with improved performance would also enable to measure directly the bubble diameter and the superheated liquid layer thickness.

4. CONCLUSIONS

The behavior of near-wall bubbles in subcooled flow boiling has been successfully observed, applying a recent digital imaging technique for R134a flow boiling under 7 bar. The main observations are summarized as follows:

(a) Discrete attached bubbles, sliding bubbles, small coalesced bubbles and large

coalesced bubbles or vapor clots are observed on the heated surface as the heat flux is increased from a low value. Significant bubble coalescence is observed for heat fluxes over ~40% CHF.

(b) The existence of a liquid sublayer under coalesced bubbles has also been identified photographically.

(c) The size of coalesced bubbles decreases with the increase in mass flux. Mass flux has no outstanding effect except for bubble size, coalescence and bubble layer.

(d) The CHF occurs during the process of periodic formation of largely vapor clots near exit.

(e) It is suggested that vapor remnants as a continuous source of bubbles, liquid sublayer depleted with bubble formation if there is not new supply of liquid, and vapor clot as an obstructer blanketing liquid supply to sublayer in high heat flux constitute the flow structure of flow boiling and characterize flow boiling phenomena.

Further investigation would be required for more reliable identification of DNB mechanisms according to various flow conditions.

Acknowledgments

This work was financially supported by the National Research Laboratory(NRL) Program of the Ministry of Science and Technology of Korea. Special thanks are given to Dr. S.Y. Chun and Dr. S.D. Hong of KAERI.

Nomenclature

G	mass flux	$kg \times m^{-2} \times s^{-1}$
T	temperature	°C
x	exit thermodynamic quality	-

Subscripts

sat saturation

References

1. F.C. Gunther, “Photographic Study of Surface-Boiling Heat Transfer to Water with Forced Convection”, *Trans. ASME*, 73 115-121(1951).

2. L.M. Jiji and J.A. Clark, “Bubble Boundary Layer and Temperature Profiles for Forced Convection Boiling in Channel Flow”, Trans. *ASME, J. Heat Transfer* 50-58 (1962).

3. Del Valle, H. Victor and D.B.R. Kenning, “Subcooled Flow Boiling at High Heat Flux”, *Int. J. Heat Mass Trans*. 28 1907-1920 (1985).
4. L.S. Tong, A.A. Bishop and L.E. Efferding, “A Photographic Study of Subcooled Boiling Flow and DNB of Freon-113 in a Vertical Channel”, *ASME paper* 66-WA/HT-3 (1966).

5. J.E. Galloway and I. Mudawar, “CHF Mechanism in Flow Boiling from a Short Heated Wall - I, Examination of Near-Wall Conditions with the Aid of Photomicrography and High-Speed Video Imaging”, *Int. J. Heat Mass Tran*. 36 2527-2540 (1993).

6. C.P. Yin, Y.Y. Yan, T.F. Lin, and B.C. Yang, “Subcooled Flow Boiling Heat Transfer of R-134a and Bubble Characteristics in a Horizontal Annular Duct”, Int. J of Heat and Mass Tran. 43, 1885-1896, (2000)

7. S.H. Chang and W.P. Baek, “Critical Heat Flux – Fundamentals and Applications”, Chungmoongak Pub. Co., Seoul, (1997) (in Korean).

8. S.H Chang and W.P. Baek, “Perspective on Critical Heat Flux Research for Reactor Design and Safety”, Proc. of the 5th Int. Top. Mtg. on Nuclear Thermal Hydraulixs, *Operations and Safety (NUTHOS-5),* Beijing, China AA1 (1997).

9. S.H Chang, I.C Bang and W.P. Baek, “Photographic Study on the Near-Wall Bubble Behavior in Subcooled Flow Boiling”, *Int. J. of Thermal Sciences,* (2002) accepted

10. C.H. Lee and I.A. Mudawwar, “A Mechanistic CHF Model for Subcooled Flow Boiling based on Local Bulk Flow Conditions”, *Int. J. Multiphase Flow*, 14 711 (1988).

11. Y. Katto, “A Physical Approach to Critical Heat Flux of Subcooled Flow Boiling in Round Tubes”*, Int. J. Heat Mass Tran*. 33, 611-620 (1990).

12. G. P. Celata, M. Cumo, A. Mariani and G. Zummo, “A Mechanistic Model for the Prediction of Water-Subcooled-Flow-Boiling Critical Heat Flux at High Liquid Velocity and Subcooling”, *Fusion Technology*, 29, 499-511 (1996).

13. J. Mitrovic, “Das Abreissen von Dampfblasen an festen Heizflachen.” *Int. J. Heat Mass Transfer* 26, 955-963 (1983).

14. P.S. Larson and L.S. Tong, “Void Fraction in Subcooled Flow Boiling”*, J. Heat Trans*. 9, 471-476 (1969).

15. C. H. Lee, I.A. Mudawwar and A. Sesonske, “A New Critical Heat Flux Model for Subcooled Two-Phase Flow through a Vertical Tube”, *Particular Phenomena and Multiphase Transprot*, Miami, 1, 425-441 (1986).

16. T.H. Chun, W.P. Baek and S.H. Chang, “An Integral Equation Model for Critical Heat Flux at Subcooled and Low Quality Flow Boiling”, *Nucl. Eng. Des*. 199, 13-29 (2000).

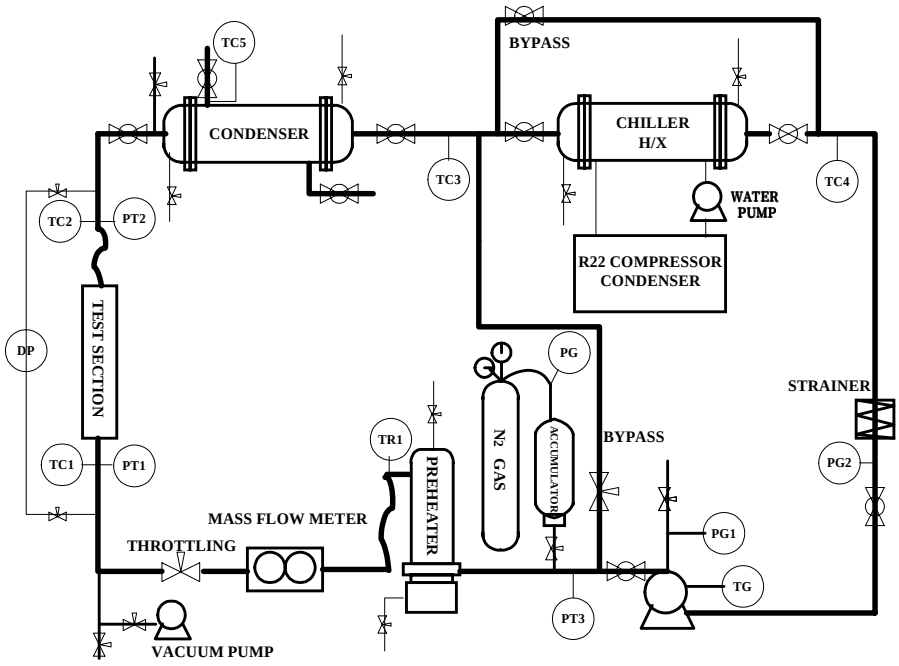

Figure 1. R134a test loop

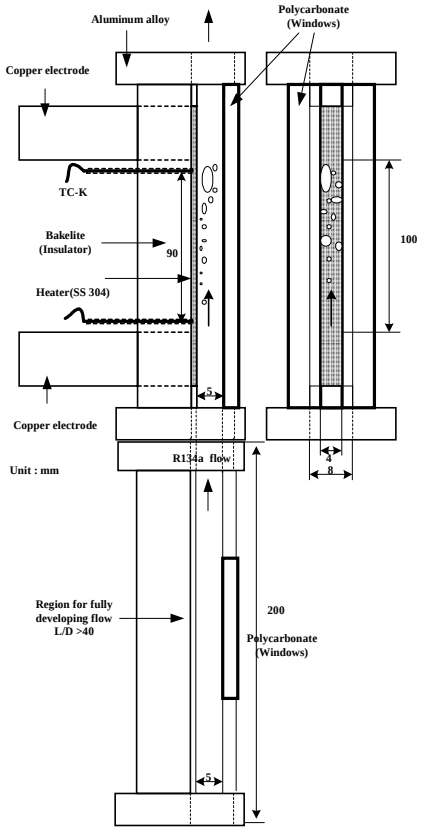

Figure 2. Test section

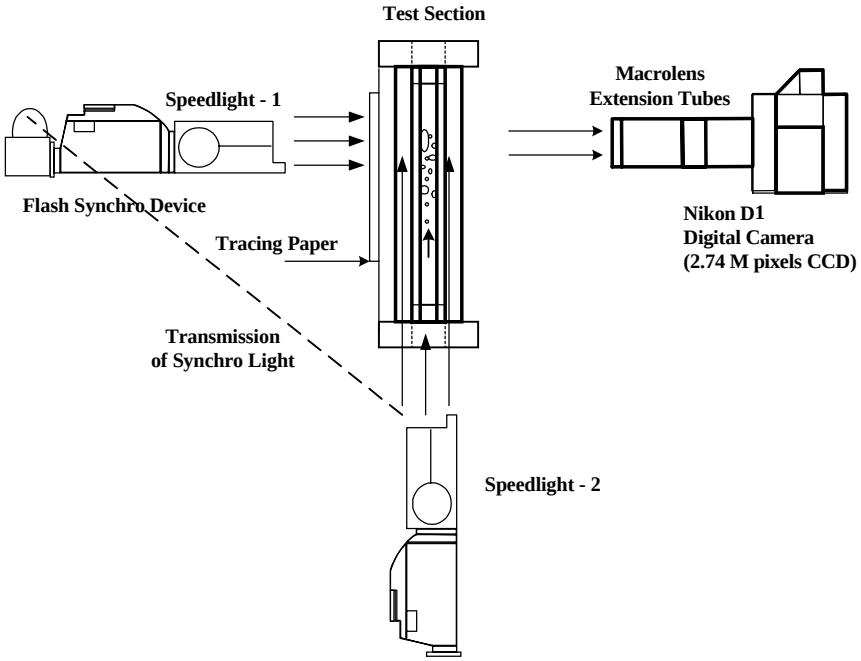

Figure 3. Photographic system

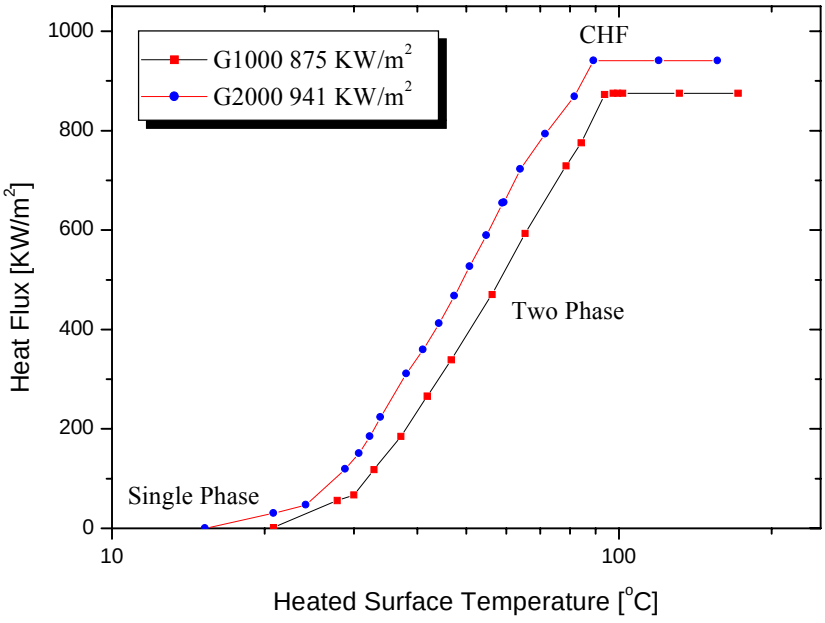

Figure 4. Boiling curves

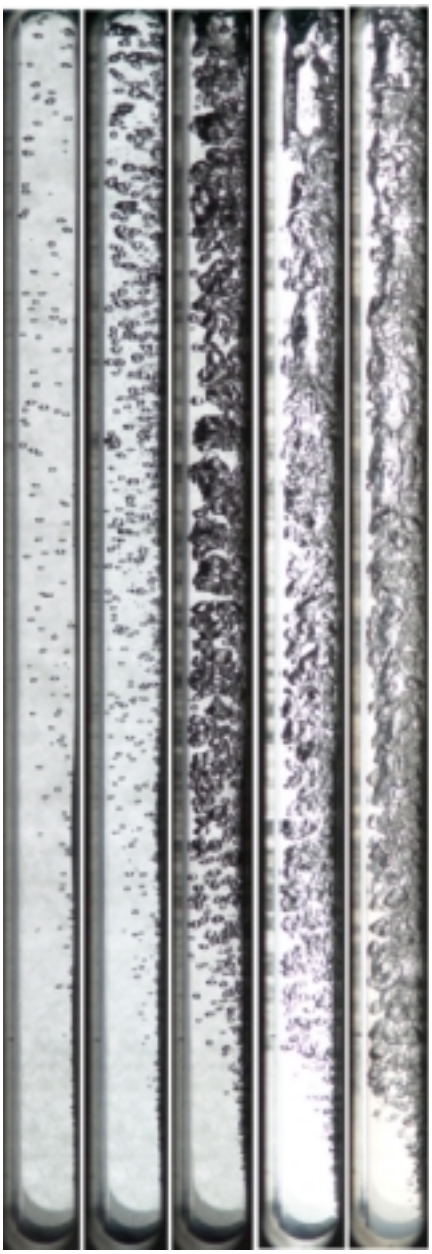

G 0 kg/m^{2}s
Lateral observation
(KW/m^2) 7.6, 17, 46, 90 , 163

Figure 5. Pool boiling

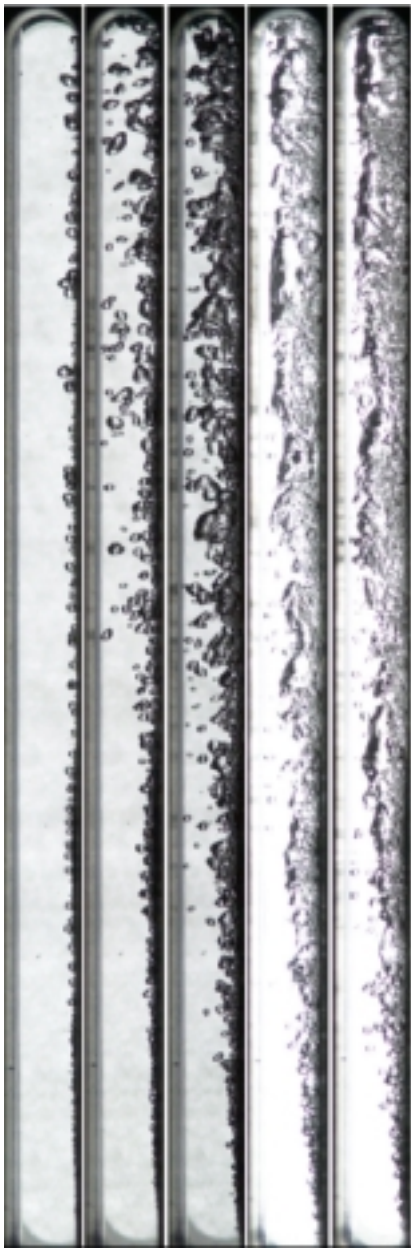

G 190 kg/m^{2}s
Lateral observation
(KW/m^2) 47, 119, 216, 360, 411
x = - 0.049, -0.028, -0.001, +0.044, +0.059

Figure 6. Boiling at low mass flux

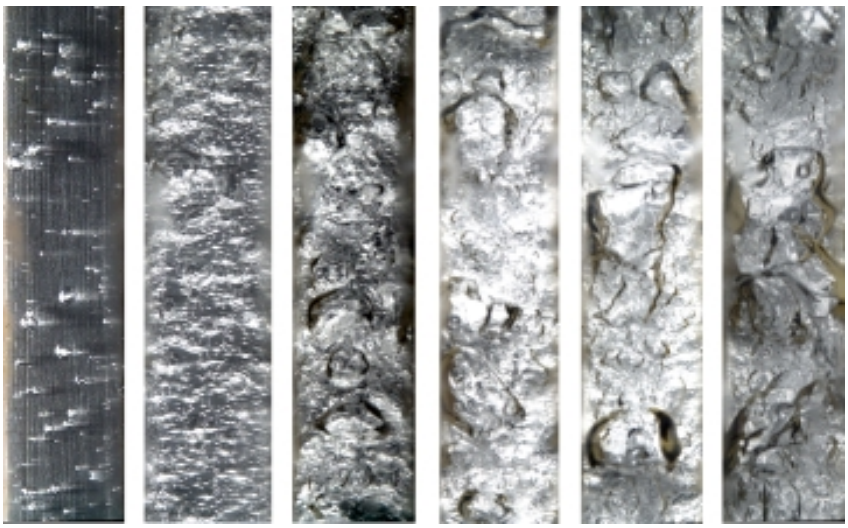

(a) G1000, Front observation
(KW/m^2) 53,142, 243, 243 , 303, 366, 477
% CHF = 6.1, 16.2, 27.8, 27.8, 34.6, 41.8, 54.5
x = -0.061, -0.055, -0.050, -0.050, -0.046, -0.043, -0.036

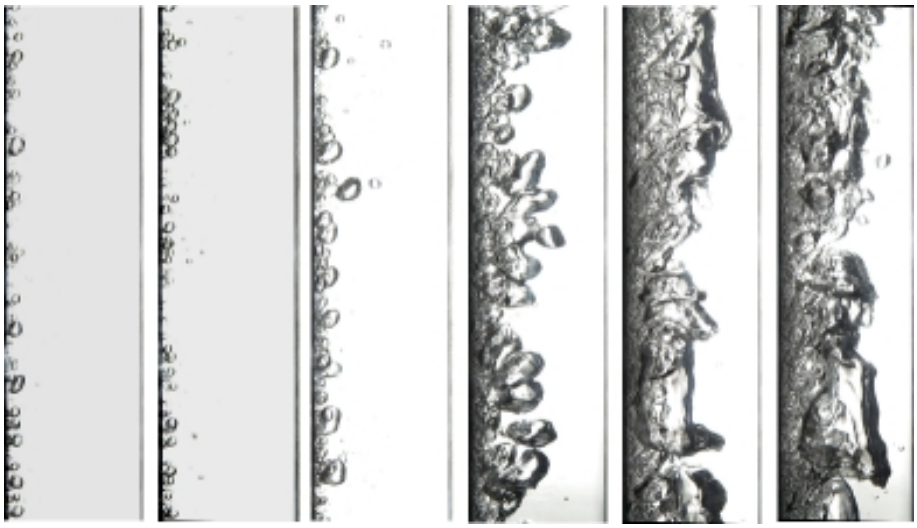

(b) G1000, Lateral observation
(KW/m^2) 82, 82, 120, 215 , 474, 670
% CHF = 9.4, 9.4, 13.7, 24.6, 54.2, 76.6
x = -0.059, -0.059, -0.057, -0.051, -0.037, -0.025

Figure 7. Bubble behavior of R134a

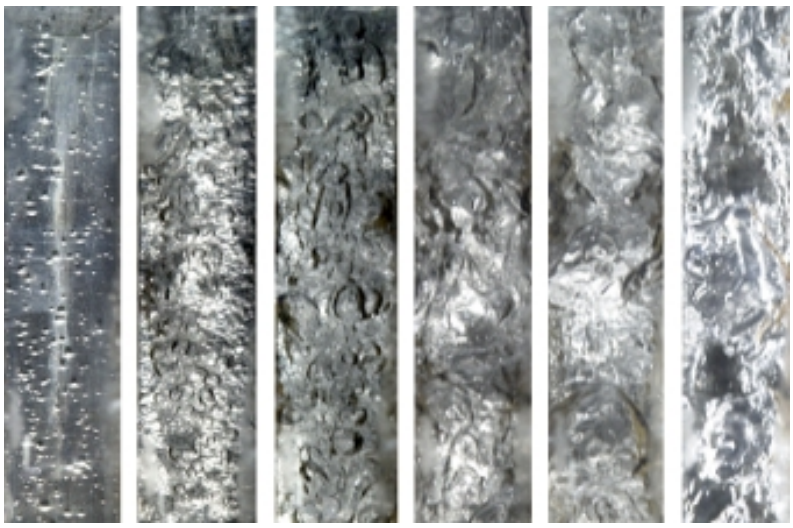

(c) G2000, Front observation
(KW/m^2) 80, 136, 295, 860, 899, 941(CHF)
% CHF = 8.5, 14.5, 31.4, 91.4, 95.5, 100
x = -0.061, -0.060, -0.055, -0.039, -0.038, -0.037

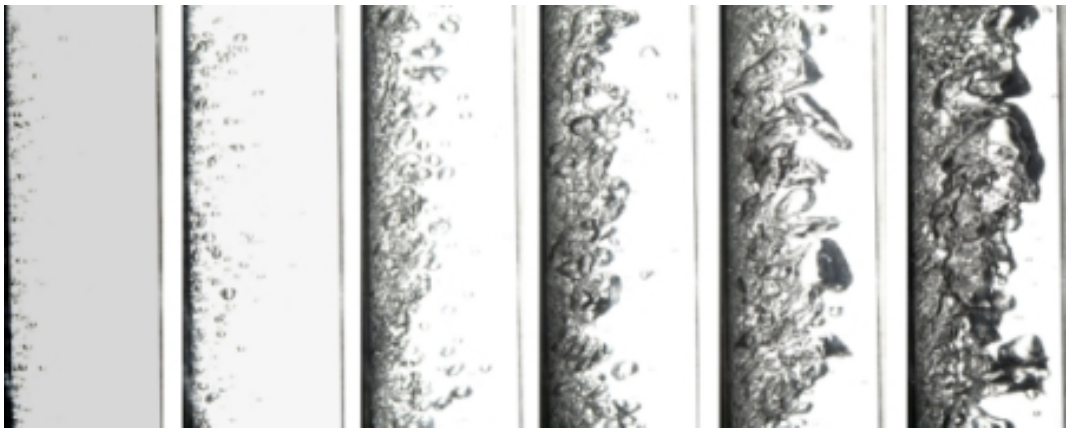

(d) G2000, Lateral observation
(KW/m^2)= 102, 120, 313, 362, 530, 941
% CHF = 10.8, 12.8, 33.3, 38.5, 56.3, 100
x = -0.061, -0.060, -0.055, -0.053, -0.048, -0.037

Figure 7. Bubble behavior of R134a

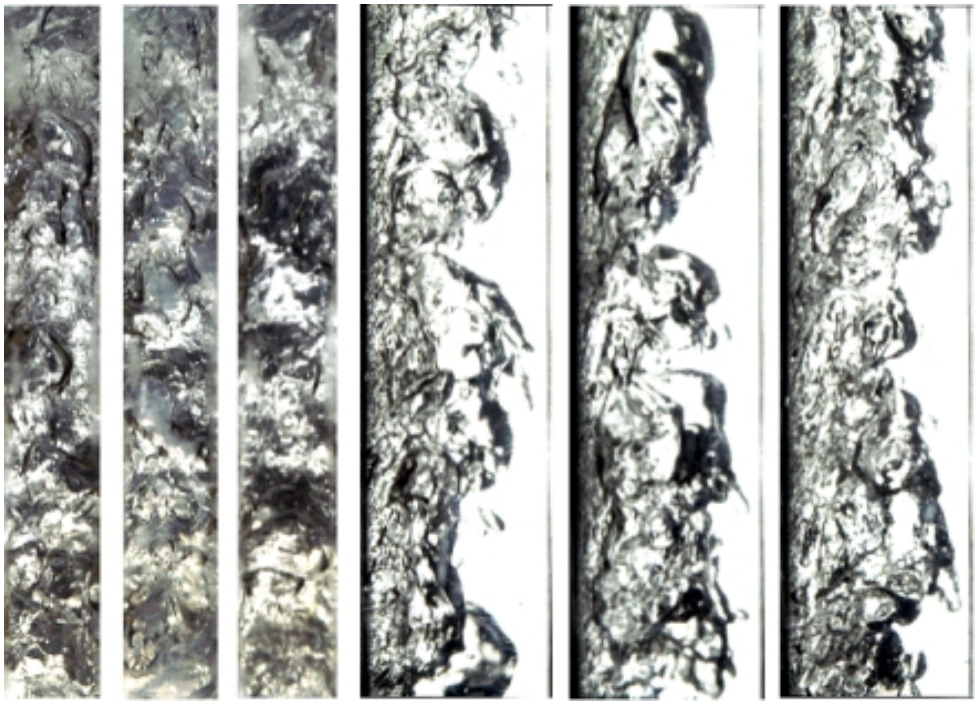

(a) Front observation (b) Lateral observation
G2000 , CHF (KW/m^2)= 941, x = -0.037

Figure 8. Flow phenomena at CHF of R134a

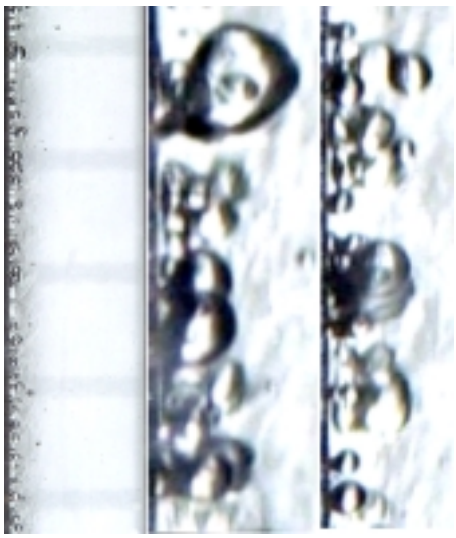

Lateral observation
First photo with 5 mm width, G 1000 kg/m^2s
82 KW/m^2 (9.4 % CHF), x = -0.059
Partially magnified two photos on the right

Figure 9. Liquid sublayer under coalesced bubbles

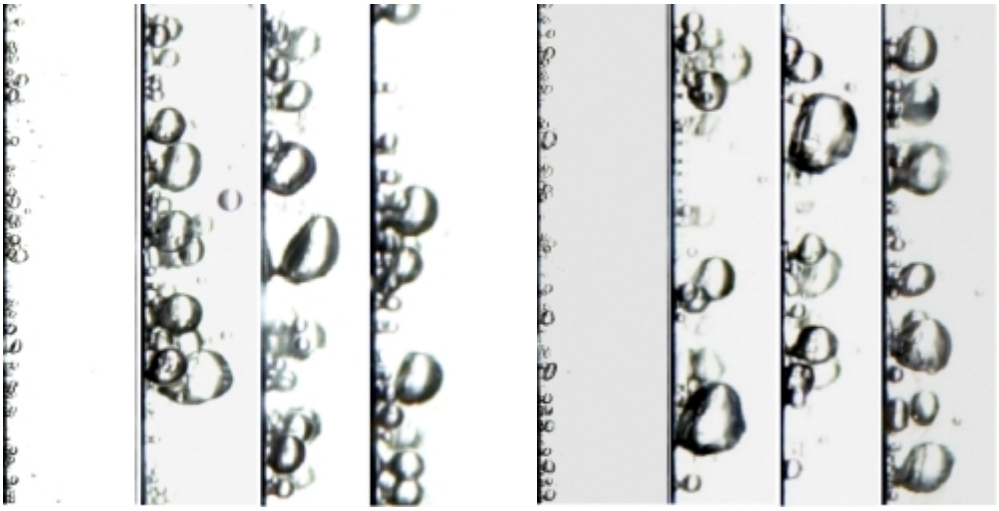

(a) Lateral observation
First photo with 5 mm width
G 1000 kg/m^{2}s
82 KW/m^2 (9.4 % CHF)
Partially magnified three photos on the right

(b) Lateral observation
First photo with 5 mm width
G 1000 kg/m^{2}s
82 KW/m^2 (9.4 % CHF)
Partially magnified three photos on the right

Figure 10. Structure of discrete bubbles on the wall

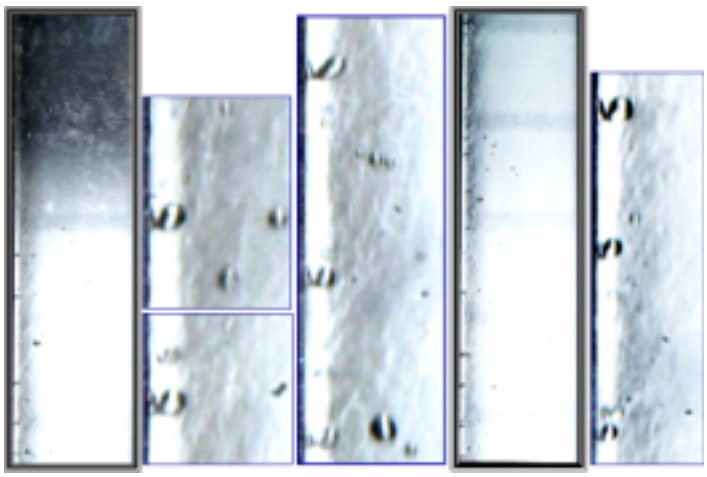

Lateral observation
Thick line photo with 5 mm width, G 2000 kg/m^{2}s
82 KW/m^2 (8.7 % CHF), x = -0.061
Partially magnified photos

Figure 11. Bubbles and vapor remnants on the wall